Scientific Research Publishing

Smart Grid and Renewable Energy, 2024, 15, 15-33
https://www.scirp.org/journal/sgre
ISSN Online: 2151-4844
ISSN Print: 2151-481X

Comprehensive Examination of Solar Panel Design: A Focus on Thermal Dynamics

Kajal Sheth[1], Dhvanil Patel[2]

[1]Department of Energy, New York Tech, Long Island, USA
[2]Petroleum Department, Texas A&M University, College Station, USA
Email: shethkajal7@gmail.com

How to cite this paper: Sheth, K. and Patel, D. (2024) Comprehensive Examination of Solar Panel Design: A Focus on Thermal Dynamics. *Smart Grid and Renewable Energy*, **15**, 15-33.
https://doi.org/10.4236/sgre.2024.151002

Received: December 29, 2023
Accepted: January 22, 2024
Published: January 25, 2024

Abstract

In the 21st century, the deployment of ground-based Solar Photovoltaic (PV) Modules has seen exponential growth, driven by increasing demands for green, clean, and renewable energy sources. However, their usage is constrained by certain limitations. Notably, the efficiency of solar PV modules on the ground peaks at a maximum of 25%, and there are concerns regarding their long-term reliability, with an expected lifespan of approximately 25 years without failures. This study focuses on analyzing the thermal efficiency of PV Modules. We have investigated the temperature profile of PV Modules under varying environmental conditions, such as air velocity and ambient temperature, utilizing Computational Fluid Dynamics (CFD). This analysis is crucial as the efficiency of PV Modules is significantly impacted by changes in the temperature differential relative to the environment. Furthermore, the study highlights the effect of airflow over solar panels on their temperature. It is found that a decrease in the temperature of the PV Module increases Open Circuit Voltage, underlining the importance of thermal management in optimizing solar panel performance.

Keywords

Solar Photovoltaic (PV) Modules, Thermal Efficiency Analysis, Open Circuit Voltage, Computational Fluid Dynamics (CFD), Solar Panel Temperature Profile

1. Introduction

As the world grapples with escalating energy demands amidst the rapid depletion of conventional fuels and rising pollution levels, the pursuit of renewable energy sources has become more critical than ever. Solar energy, with its vast and untapped potential, stands out as a key solution. It is the only renewable

energy source capable of meeting the majority of our planet's energy requirements indefinitely, making it a pivotal element in addressing global energy challenges. Solar photovoltaics (PV), a technology that efficiently converts sunlight into electricity, is at the forefront of this renewable energy revolution. It offers a sustainable solution that aligns with the goals of clean energy and environmental preservation.

Across the globe, nations are increasingly adopting solar PV, recognizing its potential to significantly contribute to their energy mix. Particularly in regions within the tropics, where sunlight is abundant, solar PV presents an unparalleled opportunity to harness this natural resource. The International Solar Alliance, comprising over 120 countries, exemplifies this global commitment. This alliance aims to mobilize USD 1 Trillion by 2030 to achieve both the Paris climate goals and the United Nations Sustainable Development Goals (SDGs), underscoring the pivotal role of solar energy in global sustainability efforts.

The economic feasibility of solar PV has seen remarkable improvements due to ongoing technological advancements. According to the National Renewable Energy Laboratory (NREL), the levelized cost of energy from solar PV has significantly decreased, from about 10 units in 2015 to approximately 3 units in 2018. Despite these advancements, challenges such as the limited efficiency of solar cells and their comparative reliability issues against fossil fuels remain. However, the long-term benefits are undeniable. For example, a 3 kW solar PV system, though initially expensive, can achieve a return on investment within three to four years. Post this period, the system generates significantly more energy than the initial investment, thanks to the solar panels' 25-year lifespan.

This paper delves into the thermal behavior of PV modules, exploring how environmental conditions and airflow over the panels affect their performance. Utilizing ANSYS Fluent v19.5 for Computational Fluid Dynamics (CFD) analysis, the study corroborates its findings with existing research and experimental setups, offering novel insights into optimizing PV module efficiency. A crucial aspect revealed is the sensitivity of PV efficiency to temperature variations, with a mere one-degree rise in module temperature potentially reducing power output by 0.4% from standard testing conditions.

As the world gravitates towards green and renewable energy sources, solar PV technology, particularly its efficiency and adaptability, stands as a pivotal area of research. This study not only underscores the critical role of solar PV in meeting global sustainable energy demands but also contributes to enhancing its practical viability and efficiency.

2. Literature Review

A photovoltaic (PV) cell is a device designed to directly transform the energy of light photons into electrical power through a single-step process. Light consists of energy packets called photons, with the energy level determined by its frequency, or the color spectrum of the light. When these photons strike the surface

of a solar cell, they influence the production of current and voltage. Solar cells, when linked together in series, form what is commonly known as a solar panel or a photovoltaic panel.

In practical applications, the most prevalent designs for solar cells are those utilizing Schottky-type metal-semiconductor-based p-n junctions.

2.1. Working of a Solar Cell

A typical solar cell, with a thickness ranging from 0.18 mm to 0.22 mm, operates based on the photovoltaic effect. This effect occurs when light of a specific energy illuminates a p-n junction, leading to the separation of excitons into electrons and holes. Within the cell's depletion region, an internal electric field causes these electrons to migrate towards different sides of the junction—the p side and the n side. When a wire is connected across the terminals, this movement of electrons results in a flow of current. Silicon-based solar cells are constructed using p-n junction diodes, which are doped with elements like boron or phosphorus. This doping process facilitates the creation of a large number of excitons that, upon exposure to light, migrate to the depletion region and then towards carrier contacts, generating an electric current in **Figure 1** below.

The individual voltage and current output of a single solar cell are typically insufficient for meeting substantial energy requirements. To address this, solar cells are interconnected in series, effectively increasing the total voltage to better cater to consumer needs. This configuration of serially linked solar cells, aimed at amplifying the system's power output, is referred to as a solar photovoltaic module. When these solar PV modules are further connected, either in series or in parallel, they form what are known as strings. The arrangement of multiple strings, whether connected in series, parallel, or a combination of both, constitutes a PV Array, which can deliver higher power outputs to meet larger energy demands.

2.2. Crystalline Silicon PV Modules

Crystalline silicon PV modules are the predominant choice in the global market, accounting for approximately 85% of market share. These modules are known for their high energy conversion efficiency, with monocrystalline cells reaching about 25% and multicrystalline/polycrystalline cells achieving over 20%. However, in industrial applications, the efficiency typically ranges from 18% to 20%.

The widespread manufacturing of silicon PV modules can be attributed to several key factors:

- Abundance: Silicon, being the second most abundant element in the Earth's crust, ensures a long-term, sustainable supply for manufacturing.
- Maturity: The semiconductor industry has an established supply chain and fabrication process for silicon chips. Adapting these existing frameworks to produce silicon-based solar cells is relatively straightforward due to the mature nature of silicon chip fabrication.

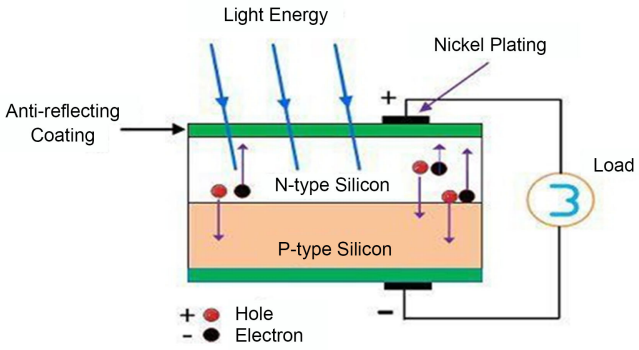

Figure 1. Working Principle of Photovoltaic Cell [1].

• Performance: Silicon PV modules offer a favorable cost-to-efficiency ratio, making them economically viable. They have proven to be the most efficient single-junction solar cells on an industrial scale.

• Reliability: Silicon PV modules are known for their longevity, typically lasting for 25 years with minimal degradation. This durability translates to a return on investment for solar PV installations within just three to four years.

In the current study, the focus is on silicon-based solar PV modules. This research aims to provide insights that industries can utilize to enhance both the efficiency and reliability of solar PV modules in practical applications.

A solar PV module is comprised of various layers, each serving distinct functions. The layout of these layers is illustrated in **Figure 2** below.

2.3. Aluminum Frame

The photovoltaic module's frame, crafted from aluminum, is strategically positioned around the module's edges to enhance its mechanical robustness. This frame includes a rubber film that ensures the secure placement of the layers and is complemented by a silicone sealant, which acts as a barrier against moisture, thus protecting the solar cells. Typically, the aluminum frame's thickness for solar modules is in the range of 0.9 mm to 1.5 mm.

The use of aluminum for these frames is particularly advantageous due to its combination of lightness and durability. This material is favored in solar panel construction for its capacity to withstand heat, its resistance to corrosion, and its ability to endure various weather conditions. These properties not only contribute to the longevity and reliability of the solar panels but also provide manufacturers with the flexibility to adapt and customize the frame shapes according to specific customer needs and preferences.

2.4. Tempered Glass

The cover glass of solar panels is designed to optimize performance, prioritizing low reflectivity, high light transmissivity, and robust strength. This glass, typically with a thickness of about 3.2 mm, is made of tempered, or toughened, glass. This kind of glass not only offers greater strength compared to standard varieties but also exhibits enhanced durability.

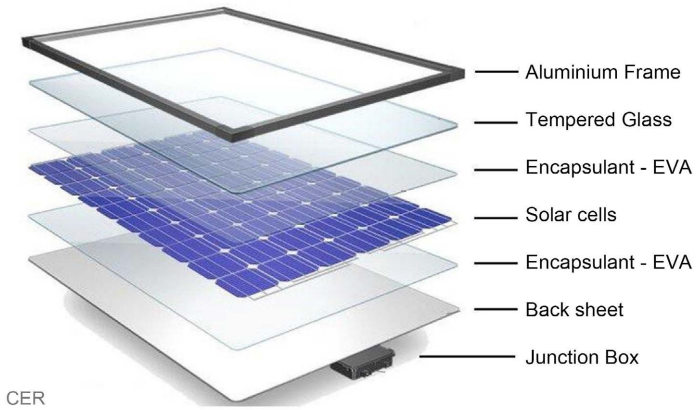

Figure 2. Solar panel construction [2].

A key feature of this glass is its textured surface, essential during the lamination process, which facilitates the effective adherence of the Ethylene-Vinyl Acetate (EVA) layer to the glass. To maximize the transmission of solar energy, manufacturers prefer using glass with a low iron oxide content, as it allows more solar energy to pass through.

Additionally, the efficiency of solar panels can be further enhanced by applying an anti-reflective coating. This is achieved by layering a film of anti-reflective material onto the glass before it undergoes the tempering process. Such coatings are significant as they can increase solar irradiance absorption by over 2.5%. In practical terms, this enhancement could mean an increase of more than 6 W in peak power for a solar module rated at 250 Wp, thereby boosting the overall power generation efficiency of the solar panel.

A UV trapping layer on the rear surface of solar panels selectively allows radiation through while blocking harmful UV rays, thereby protecting and optimizing solar cell performance in **Figure 3** below.

2.5. Encapsulant-EVA

Solar cells and their interconnects are fully encapsulated with Ethylene-Vinyl Acetate (EVA), ensuring the cohesive bonding of all components. EVA, a Polyolefin polymer, is selected for its weather resistance, high optical transmission, and durability, all achieved cost-effectively. While Polyvinyl Butyral (PVB) is also utilized, it presents certain limitations in UV and IR ray protection, though recent advancements have mitigated these issues, making it more viable for industry use. These polymers possess viscoelastic properties, leading to changes in viscosity and elasticity based on temperature and time. Such changes can impact the thermal mechanics of the module, especially at temperatures above 75˚C.

2.6. Backsheet

The rear side of the module is equipped with a protective layer designed to mitigate environmental impacts from UV rays and moisture. Utilizing multi-layered polymeric back-sheets, this layer offers enhanced thermal dissipation compared

to glass. Materials like PET (Polyethylene Terephthalate), PVF (Polyvinyl Fluoride), and epoxy silane are commonly used in the composition of these protective layers in Figure 4 below.

2.7. Interconnects

To connect solar cells, ribbons made of highly conductive materials such as copper are employed. These ribbons, varying in thickness from 0.2 to 0.5 mm, are crucial for establishing cell-to-cell connections. The joining process involves using SnPb (tin-lead) or lead-free solder alloys to connect the outer surface of one cell to the rear surface of an adjacent cell. This configuration allows for the efficient transfer of current from one cell to another, arranging them in a series. It is important to note that the process must be handled meticulously, as stresses often develop in these interconnects, which could affect the overall integrity and performance of the solar module.

2.8. Junction Box

The junction box, serving as the housing for electrical connections, is mounted on the back side of the PV module. It is typically adhered to the backsheet using silicone sealant glue for secure attachment. If this junction box fails, it can cause sparks and arcs, representing a significant safety hazard and posing a serious risk to the integrity and functioning of the PV module.

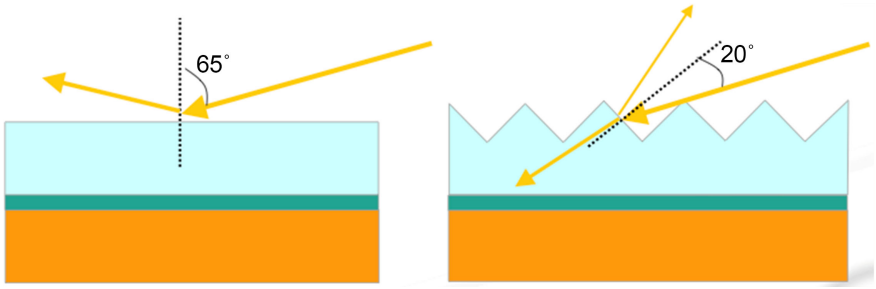

Figure 3. Standard solar glass (on left) vs light trapping [3].

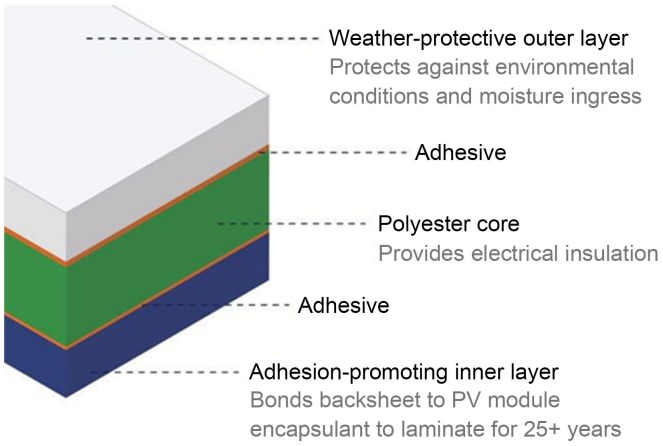

Figure 4. Multilayer backsheet structure [4].

2.9. Thermal Analysis of PV Modules

Solar photovoltaic technology primarily relies on silicon, a semiconductor material, to convert solar energy into electrical power. This process involves the generation of electron-hole pairs within the silicon, which then travel to metal contacts and are subsequently directed to loads through busbars. However, the efficiency of these solar panels is a significant concern, as it is capped at a maximum of about 25% in ground-based applications.

Research has demonstrated that the efficiency of solar panels can be affected by temperature. Specifically, cooling the panels can enhance their efficiency, while heating them tends to decrease it. This variation is due to the changes in the width of the depletion layer, which is sensitive to temperature fluctuations. For every degree of increase in the module's temperature, the power output of the PV module drops by approximately 0.4% from its rated power under Standard Test Conditions (STC) in **Figure 5** & **Figure 6**.

Previous research on thermal models for photovoltaic (PV) modules, which employed thermal and energy balance equations, includes work by Faiman [7], Shoplaki [8], Mattei [9], and King [10]. These studies, however, encountered limitations due to their focus on specific locations, module configurations, solar cell materials, or encapsulation data, leading to varying heat transfer coefficients. Additionally, the impact of airflow over the PV module was often not considered in these analyses.

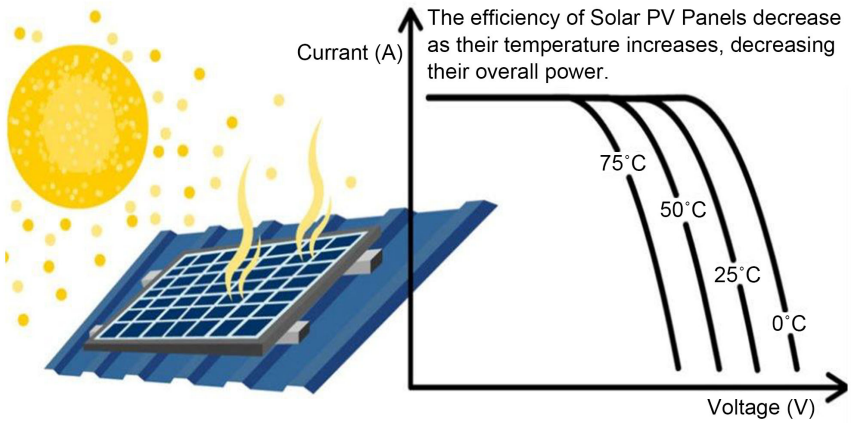

Figure 5. Effect of temperature on solar PV panels [5].

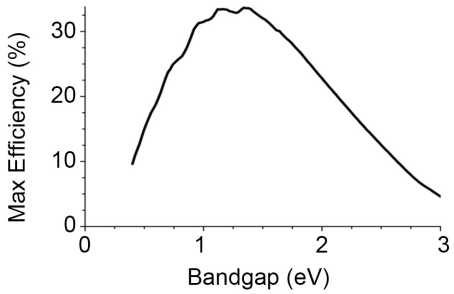

Figure 6. Shockley Queisser limit [6].

Addressing these gaps, Lee and Tay [10] conducted numerical simulations using Finite Element Method (FEM) to map the temperature distribution across different layers of a PV module. Similarly, Usama Siddiqui *et al.*, in 2012 [11], investigated how environmental temperature and solar irradiance affect PV module performance. More recently, Zhou *et al.* [12] analyzed the thermal conditions and temperature profiles of PV modules, specifically considering the solar radiation absorption by each layer.

Despite the detailed insights offered by FEM simulations, their resource-intensive and time-consuming nature has made them a less favored method for analyzing the thermal conditions of PV modules. Consequently, using FEM to simulate the thermal profile under varied ambient conditions for a PV module presents significant challenges.

3. Methodology

In this study, we have conducted a Computational Fluid Dynamics (CFD) Thermal Analysis of a PV Module using ANSYS Fluent. Our focus was on understanding how variations in velocity, irradiation level, and ambient temperature conditions affect the temperature profile of a PV Module. We aim to derive the heat transfer coefficient for the PV Module based on its average performance, and then validate this through various experiments, including Infrared (IR) Thermography. This approach is intended to aid in the tailored manufacturing of Solar Panels, optimizing power generation and customer benefits based on the specific deployment location.

CFD has been an instrumental tool in this simulation, allowing us to consider the turbulence caused by air flowing over the PV module, the irradiation impacting the Solar PV Module, and the optical activities of transmission, absorption, and reflection. The simulation also accounts for heat transfer processes including conduction, convection, and radiation between the different layers of the module. Layer properties are based on standard data from similar research. Using ANSYS Fluent, the simulation sets inlet and outlet boundary conditions, along with air velocity and environmental conditions. It results in a detailed temperature profile for each layer of the PV Module. Subsequently, the area-weighted mean temperature of these layers is calculated, followed by the determination of the heat transfer coefficient using Newton's Law of Cooling.

Environmental Boundary Conditions for the simulation include:

1) Analysis of the average temperature across the various layers of the PV Module, considering that insolation is primarily responsible for the temperature rise.

2) The PV Panel, placed within an enclosure filled with fluid (air), allows airflow at varying velocities over the panel, which is inclined at 30 degrees.

3) The input conditions for the simulation are summarized as follows: The insolation on the Solar Panel is assumed to be 1000 W/m^2, with an Ambient Temperature of 298 K. The absorption of solar energy in different layers is based on data from PV Lighthouse, consistent with conditions referenced in a related thesis in shown **Table 1**.

Table 1. Properties of various layers of PV module [13].

Different parts of the module	Thickness (in mm)	Thermal conductivity (W/mK)	Specific heat capacity (J/kgK)	Density (kg/m^3)	Refractive index	Emissivity	Solar energy absorbed (in W/m^2)
Glass	3.2	0.8	800	2500	1.486	0.85	38.0
EVA	2.4	0.34	1400	950	1.503	-	7.5
Silicon	0.18	130	700	2329	3.44	-	834
Backsheet	1.0	0.1583	1760	1720	1.334	0.9	13
Aluminium	2.0	202.4	871	2719	3.0823	0.71	800

3.1. Heat Transfer Assumptions

In the simulation, the silicon, and Ethylene-Vinyl Acetate (EVA) layers of the solar panel are observed to heat up primarily due to thermal conduction. This is attributed to their higher thermal conductivity relative to other layers in the panel. However, components with low thermal mass, such as interconnects like copper bridges or busbars, have been excluded from the simulation because their impact on overall thermal behavior is considered negligible shown in **Table 2**.

3.2. Governing Equations & Models

The analysis in this study utilizes various models, each governed by specific equations. These governing equations have been instrumental in formulating and deriving the results of the analysis.

3.2.1. Realizable k-ϵ Model

To address the challenge of high Reynolds stresses in the Reynolds-Averaged Navier-Stokes (RANS) equations, the Boussinesq hypothesis is employed, which necessitates the calculation of eddy viscosity. This viscosity can be determined using the mixing length concept, a method that relies on turbulence kinetic energy (k) and its dissipation rate (ϵ) for flows.

The transport equation for k is solved using the Realizable k-ϵ model, and a separate transport equation is utilized for the dissipation rate ϵ. By obtaining values for both k and ϵ, the eddy viscosity term can be accurately calculated. This term is crucial for the closure of the RANS equations.

The Realizable k-ϵ model is particularly effective for various types of flows, including planar and round jet flows, those involving rotation, boundary layer flows, and flows under adverse pressure gradients. The model is defined by the following transport equations:

$$\frac{\partial}{\partial t}(\rho k)+\frac{\partial}{\partial x_j}(\rho k u_j)=\frac{\partial}{\partial x_j}\left[\left(\mu+\frac{\mu}{\sigma_k}\right)\frac{\partial k}{\partial x_j}\right]+G_k+G_b-\rho\epsilon-Y_m+S_k$$

and

$$\frac{\partial}{\partial t}(\rho\epsilon)+\frac{\partial}{\partial x_j}(\rho\epsilon u_j)$$
$$=\frac{\partial}{\partial x_j}\left[\left(\mu+\frac{\mu_t}{\sigma_\epsilon}\right)\frac{\partial_\epsilon}{\partial x_j}\right]+\rho C_1 S_\epsilon-\rho C_2\frac{\epsilon^2}{k+\sqrt{\nu\epsilon}}+C_{1\epsilon}\frac{\epsilon}{k}C_{3\epsilon}G_b+S_\epsilon$$

Table 2. Modes of heat transfer for various layers [13].

	Conduction	Convection	Radiation
Aluminum Frame	No	Yes	Yes
Tempered Glass	No	Yes	Yes
Encapsulant-EVA	Yes	No	No
Solar Cells	Yes	No	No
Encapsulant-EVA	Yes	No	No

where,

$$C_1 = \max\left[0.43, \frac{\eta}{\eta+5}\right], \quad \eta = S\frac{k}{\epsilon}, \quad S = \sqrt{2S_{ij}S_{ij}}$$

G_k—The generation of turbulence kinetic energy due to the mean velocity gradients.

G_b—Generation of turbulence kinetic energy due to buoyancy.

Y_m—The contribution of the fluctuating dilatation in compressible turbulence to the overall dissipation rate.

σ_k and σ_ϵ—Turbulent Prandtl numbers for k and ϵ.

S_k and S_ϵ—User defined source terms.

3.2.2. Energy Equations

According to the first law of Thermodynamics, the rate of change in the total energy of a system equals the net energy transfer into or out of the system. This energy transfer includes heat generation from sources, work transfer (encompassing both viscous and pressure work), and net heat transfer across the system's boundaries.

In the context of low-speed flows, the total energy per unit mass can be effectively related to temperature by using the concept of enthalpy, represented as $h(T)$. This relationship allows for the transformation of the energy equation into a temperature equation. This approach is applicable to both solids and liquids, with the modification that the internal energy change (U) is considered zero for solids.

Furthermore, this formulation is not restricted to incompressible fluids; it is also applicable to compressible fluids. In such cases, both conduction and convection are significant factors in the energy equation, playing major roles in the transfer and distribution of energy within the system.

$$\frac{\partial(\rho e_t)}{\partial t} + \nabla\cdot\left[\vec{V}(\rho e_t + p)\right] = \nabla\cdot\left[k\nabla T + \left(\bar{\bar{\tau}}\cdot\vec{V}\right)\right] + \dot{S}_g$$

e_T—Total energy of system

$K\Delta T$—Heat transfer through conduction

$\tau\cdot V$—Viscous work

S_g—Source term of energy

$p\cdot V$—Pressure work

3.2.3. Discrete Ordinates Model

The Discrete Ordinates Model is a sophisticated radiation model employed for simulating solar irradiance impacting a Solar PV Panel. This model not only accounts for the solar irradiance but also factors in the properties of the air when determining the heat flux on the PV Panel. It is especially beneficial in scenarios where the gas (in this case, air) is a participant in the radiation process.

One of the model's core functionalities is solving the Radiation Transport Equation. This involves considering the effects of absorption, emission, and scattering integral in the radiation process. These effects are analyzed along specified beam directions (s) and at various angular positions of intensity (Ω) that strike the module.

A distinctive feature of this model is its ability to discretize radiation intensities into spheres divided into octants. This approach enables the precise calculation of radiation intensities at specific points. To accurately ascertain the intensity at any given point (I_λ), it is imperative to have detailed information on several key parameters: the absorption coefficient (a_λ), the scattering coefficient (σ_s), and the refractive index of air (n) as it interacts with the PV Module. These factors are crucial in accurately modeling and analyzing the interaction of solar radiation with the panel and the surrounding air, leading to a comprehensive understanding of the radiation effects on the performance of the PV Module.

$$\nabla \cdot \left(I_\lambda\left(\vec{r},\vec{s}\right)\vec{s}\right)+\left(a_\lambda+\sigma_s\right)I_\lambda\left(\vec{r},\vec{s}\right)=a_\lambda n^2 I_{b\lambda}+\frac{\sigma_s}{4\pi}\int_0^{4\pi} I_\lambda\left(\vec{r},\vec{s}'\right)\Phi\left(\vec{s}\cdot\vec{s}'\right)\mathrm{d}\Omega'$$

3.2.4. Navier-Stokes Equation

The Navier-Stokes equation represents Newton's Second Law of Motion adapted into partial differential form to describe the flow dynamics of incompressible and frictionless fluids. This equation essentially characterizes how fluids respond to various forces, including pressure, viscous forces, and gravity. It intricately details the relationships between key fluid properties such as velocity, pressure, temperature, and density, providing a comprehensive framework to understand and predict the behavior of moving fluids under different physical conditions.

$$\frac{\partial u}{\partial t}+u\nabla u=-\frac{\nabla P}{\rho}+\nu\nabla^2 u$$

u—fluid velocity vector, P—fluid pressure, ρ—fluid density, ∇^2—Laplacian operator.

3.2.5. Continuity Equation

The continuity equation is fundamentally based on the principle of mass conservation. This principle asserts that for a fluid in motion, such as air flowing over a PV panel, the mass within any given volume must remain constant over time. Therefore, the equation implies that the time rate of change of the density of the fluid element (in this case, air) is zero, meaning there is no accumulation or loss of mass in any part of the flow field. This is a key concept in fluid dynamics, ensuring that the mass of the fluid is conserved as it moves and interacts

with structures like a PV panel.

$$\frac{D\rho}{Dt} + \rho\nabla \cdot \vec{v} = 0$$

ρ—fluid density, V—fluid velocity.

3.3. Simulation Setup

To effectively analyze the PV Module, a systematic approach is followed, which involves several key steps:

1) Creating the Geometry: Initially, the geometry of the PV Module is sketched based on the specifications illustrated in Figure 7. This step involves accurately replicating the dimensions and layout of the PV Module.

2) Enclosure Setup: Next, the PV Module is positioned within an enclosure. This setup is crucial for defining the inlet, outlet, and wall conditions for the simulation. This arrangement is detailed in Figure 8.

3) Enclosure with Defined Conditions: The geometry is then enclosed within an environment that facilitates the interaction between the solid (PV Module) and the fluid (air) within the enclosure. This interaction is critical for the simulation and is represented in Figure 9.

4) Meshing the System: The meshing process follows, where the solar panel and the surrounding enclosure are meshed using tetrahedron type elements with fine settings. This meshing is crucial for the accuracy of the simulation. The meshing detail is shown in Figure 10.

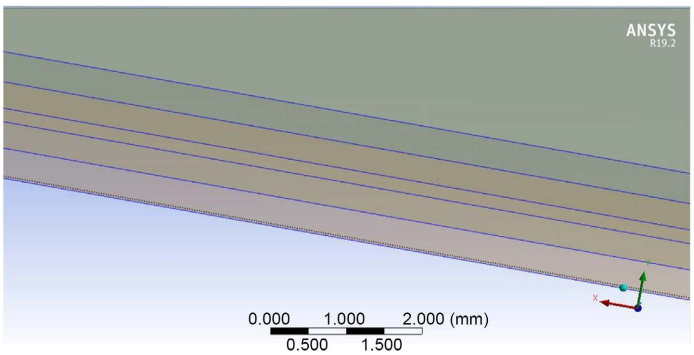

Figure 7. Geometry of PV Module.

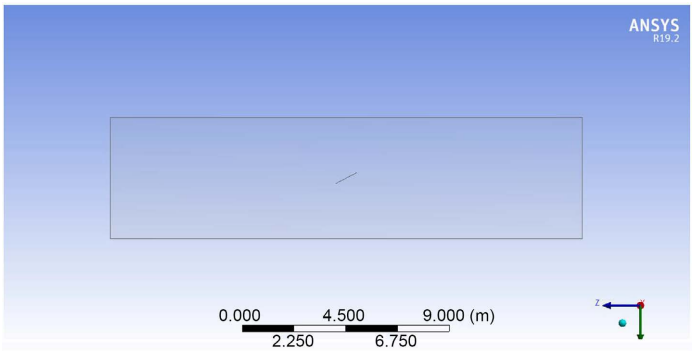

Figure 8. Solar PV Module inside an enclosure.

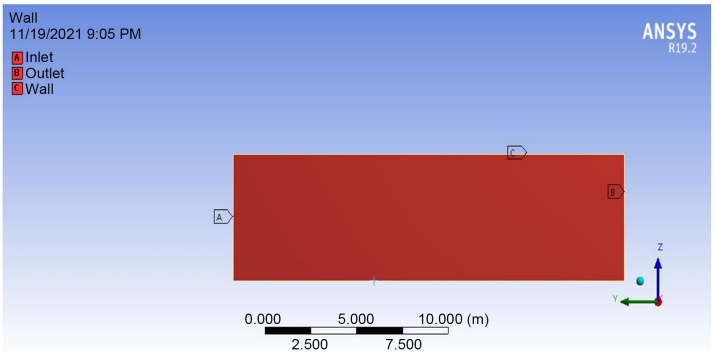

Figure 9. Solar PV Module inside an enclosure with inlet and outlet conditions.

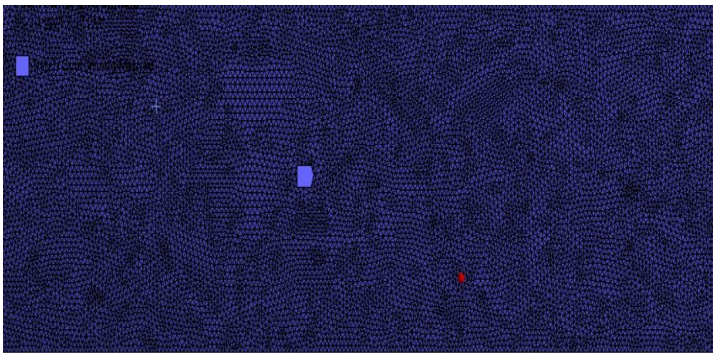

Figure 10. Meshing of system.

5) Meshing Statistics: The final mesh comprises 103,079 nodes and 516,942 elements. These figures indicate the complexity and detail of the mesh, which is vital for the precision of the computational analysis.

Each of these steps plays a critical role in setting up the simulation environment, ensuring that the analysis of the PV Module under various conditions can be conducted with high fidelity.

3.3.1. Grid Independence Study

The Grid Independence Study for the solar PV Panel mesh aims to evaluate the consistency of temperature readings across various layers of the module under a fixed initial condition of 25˚C and an air velocity of 0 m/s. The study's goal is to determine if further refinement of the mesh (beyond a 0.6% improvement) significantly alters the temperature outcomes for the backsheet, EVA, silicon, and glass layers of the PV Module.

The results indicate that temperatures across these layers remain consistent to one decimal place, even with incremental mesh improvements. This consistency suggests that the mesh is sufficiently refined for accurate simulation results shown in **Table 3**.

3.3.2. Boundary Conditions

For the simulation setup, the following boundary conditions were considered:

- Gravity: The acceleration due to gravity is set in the z-direction at 9.81 m/s^2.

Table 3. Grid independence study of meshing used for PV Module.

S. No	Nodes	Elements	Temp of Backsheet	Temp of EVA	Temp of Silicon	Temp. of Glass
1	104,110	522,111	316	316	316	316
2	105,140	527,281	315	315	315	315
3	106,171	532,450	315	315	315	315
4	107,202	537,619	315	315	315	315
5	108,233	542,789	315	315	315	315
6	109,264	547,958	315	315	315	315

• Radiation Model: The Discrete Ordinates Model is used for simulating radiation.

• Radiation Intensity: The radiation intensity is assumed to be 1000 W/m^2.

• Energy Equation: The energy equation is activated for the simulation.

• Inlet Velocity: Different velocity conditions are set at the inlet.

• Simulation Method: The Realizable k-epsilon model is used for standard wall conditions.

These boundary conditions are integral to accurately mimicking the physical environment and ensuring the reliability of the simulation results.

4. Results and Analysis

4.1. Grid Independence Study

This study investigates the effect of air velocity and heat generation on the temperature profile of a Solar PV Module's various layers. We obtained the average temperature of these layers using a weighted area average under surface integral. Based on this, we calculated the average heat transfer coefficient for the PV Module.

Case 1: Heat Generation in Silicon Layer Only

Observations indicate that after a 0.6% improvement in the mesh, the temperature of the backsheet, EVA, silicon, and glass remains constant, as shown in Table 4.

Case 2: Heat Generation in All Layers

We analyzed the heat absorption in various layers with the following results in Table 5.

Heat Absorption in various layers is as follows

1) In Si, it is 834 W/m^2

2) In Glass, it is 38 W/m^2

3) In EVA, it is 7.5 W/m^2

4) In Backsheet, it is 13 W/m^2

Heat Transfer Coefficient per unit area for Si layer when there is heat generation in only Si layer,

At air velocity = 0 m/s, $h_{conv} = \frac{834}{T_{surf} - T_a} = \frac{834}{312.2027 - 298} = 58.722 \frac{\text{W}}{\text{m}^2 \cdot \text{K}}$

Table 4. Results for heat generation in Si layer only.

Irradiation	Air Velocity (m/s)	Backsheet Temp. (K)	Silicon Temp (K)	EVA Temp (K)	Glass Temp (K)	Heat Absorption in Si (W/m^3)	Heat Absorption In W/m^2
1000 W/m^2	0	312.071	312.2027	312.1699	312.0204	463,333	834
1000 W/m^2	1	301.4384	301.5624	301.5321	301.3993	463,333	834
1000 W/m^2	2	302.2078	302.2051	302.2051	302.2062	463,333	834

Table 5. Results for heat generation in all layers.

Irradiation	Air Velocity	Back sheet Temp (K)	Silicon Temp (K)	EVA Temp (K)	Glass Temp (K)
1000	0	315.0878	315.2222	315.1903	315.0535
1000	1	299.4472	299.4623	299.4581	299.4637
1000	2	298.6801	298.6848	298.6827	298.696

Heat Transfer Coefficient per unit area for Si layer when there is heat generation in all layers,

At air velocity = 0 m/s, $h_{conv} = \frac{834}{313.2222 - 298} = 54.7884 \frac{\mathrm{W}}{\mathrm{m}^2 \cdot \mathrm{K}}$

Figure 11 shows the total temperature conditions across the PV Module.

The temperature profiles across the various layers of the solar PV Module exhibited minimal variation, as indicated by the data in the above table. Due to this negligible difference in temperatures across the layers, detailed graphical representations of these profiles have not been included in the above section.

4.2. Experimental Validation

For the experimental study, a comprehensive approach was employed involving various instruments:

1) Digital Pyranometer: This was used to measure solar irradiance, providing a quantitative assessment of the sunlight intensity impacting the Solar PV Panel.

2) Weather Station: This tool helped in determining the speed of air flowing over the Solar PV Panel. Air velocity is a crucial factor in understanding the cooling effect on the panel.

3) IR Thermograph: This device was instrumental in measuring the temperature at various points on the Solar PV Panel. For simplicity and effectiveness, temperatures were recorded at three key locations: the first endpoint, the midpoint, and the second endpoint of the panel.

The experimental study was conducted under specific environmental conditions:

- Ambient Temperature (Ta): 20˚C
- Time: 2:35 PM
- Relative Humidity (RH): 37%

We have found the following observations in Table 6 below.

Figures 12-14 show IR Thermograph readings for different points on the panel.

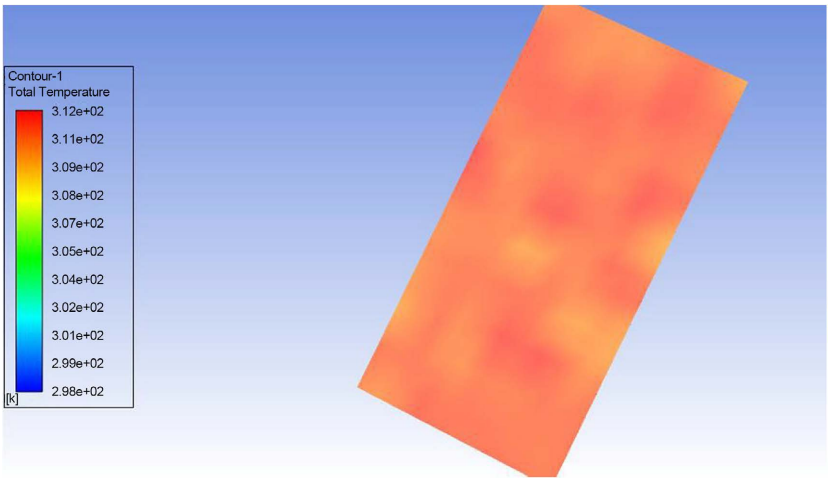

Figure 11. Temperature profile of Si layer.

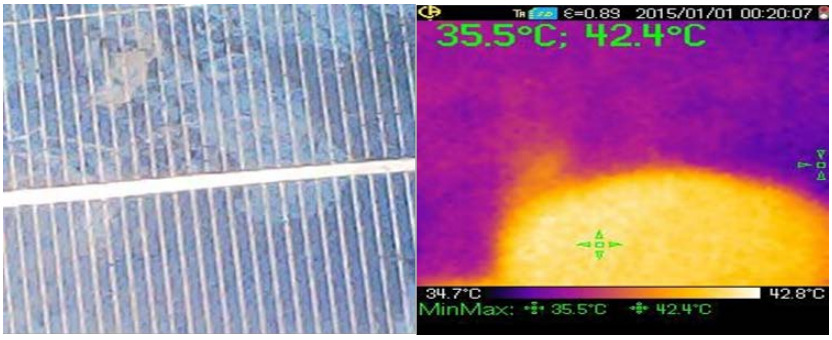

Figure 12. IR thermograph reading for Endpoint 1.

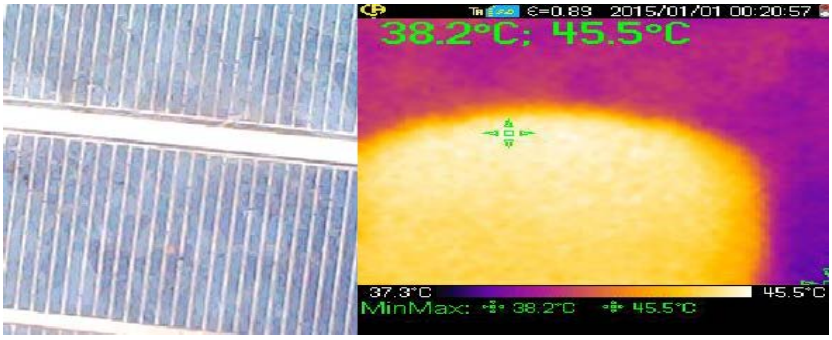

Figure 13. IR thermograph reading for Midpoint.

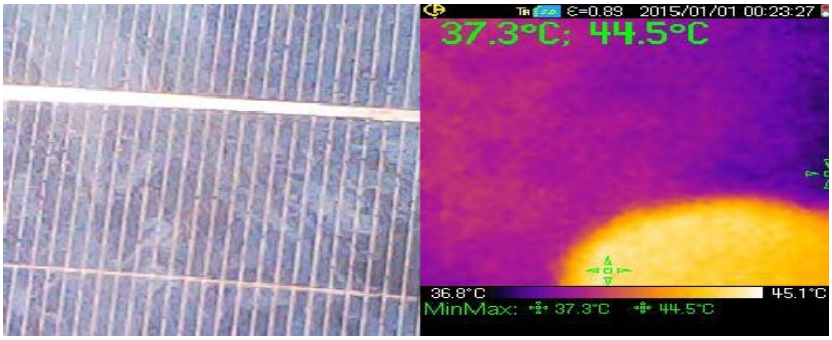

Figure 14. IR thermograph reading for Endpoint 2.

Table 6. Experimental observations.

Irradiation (W/m^2)	Efficiency (%)	Endpoint 1 Temp (˚C)	Midpoint Temp (˚C)	Endpoint 2 Temp (˚C)	Avg. Temp (˚C)	WS (m/s)
804	7.758	42.4	45.5	44.5	44.13	2.5
730	7.132	45.1	46	45.1	45.4	0.833
717	6.998	44.2	46.3	44	44.8	833
715	6.950	39.7	45.5	45.6	43.6	1.667
706	6.850	43.6	45.3	41.7	43.53	0.55

4.3. Interpretations

Based on the experimental study, several key interpretations can be drawn:

• Temperature Difference Correlation: The study revealed that the temperature difference between the PV Module and the surrounding environment is approximately 25.1˚C under conditions of 723.5 W/m^2 irradiance and an air velocity of 0.833 m/s. In contrast, the simulation results indicated a temperature difference of about 15˚C at a higher irradiance of 1000 W/m^2 and a wind speed of 0 m/s.

• Simulation Validity: Given these observations, it can be inferred that the simulation is approximately 70% accurate compared to a more generalized extrapolated value of 22˚C. This assessment reflects the simulation's effectiveness in capturing the real-world behavior of the PV Module under varying environmental conditions, albeit with some deviations that might be attributed to factors not accounted for in the simulation.

4.4. Analysis

The extensive thermal analysis conducted on the Solar PV Module, considering variations in wind speed and solar irradiance, has provided several valuable insights:

1) Wind Speed Impact: Increasing wind speed leads to a temperature drop across various layers of the PV Module, reducing the temperature difference between the PV Panel and its surroundings by approximately 2˚C. This suggests that higher wind speeds can help dissipate heat from the module more effectively.

2) Temperature Differential: In cases where there is no wind blowing over the panel, the temperature differential between the PV Panel and its surroundings remains at approximately 17 K. This implies that factors other than wind speed, such as solar irradiance, have a significant influence on temperature variations.

3) Turbulence Challenges: Practical scenarios involving turbulent air flow over the solar panel are challenging to model accurately. Consequently, some discrepancies were observed between the experimental case and the simulation study, highlighting the complexities of accounting for real-world turbulence effects.

4) Moisture Considerations: Notably, the simulation did not account for the

effect of moisture on the solar PV Panel. Moisture can potentially have a detrimental impact on the temperature profile of the panel. Future simulations or studies may need to incorporate moisture effects for a more comprehensive analysis.

Overall, this analysis underscores the importance of considering multiple factors, including wind speed, solar irradiance, and turbulence, in the thermal analysis of solar PV Modules. Additionally, addressing the influence of moisture can further enhance the accuracy of such studies.

5. Conclusions

In our comprehensive study focusing on the thermal and structural analysis of PV modules, we have conducted simulation studies to address key real-world challenges faced by solar panels in their operational environments. Our aim was to enhance both the efficiency and reliability of PV modules for long-term performance.

For the thermal analysis, we utilized CFD Fluent, maintaining a solar panel tilt angle equal to the latitude angle of the geographical location of interest. Realistic air flow over the solar panels was simulated, while environmental temperatures were kept constant. We considered irradiation levels based on STC conditions and employed various CFD models, including the discrete ordinates model, K epsilon turbulence model, and fundamental CFD equations.

Our findings revealed a temperature gradient across the layers of the PV module, primarily driven by conduction, with an approximate temperature difference of 2 degrees Celsius. Additionally, we observed a temperature differential of about 22 degrees Celsius between the solar PV panel and its surrounding environment during normal sunshine hours.

Furthermore, our simulation studies demonstrated that increasing air flow velocity over the PV panel led to a decrease in temperature across all layers of the panel. This reduction in temperature directly contributed to an improvement in the efficiency of solar panels due to an increase in the bandgap of the solar cells.

Overall, our research provides valuable insights into addressing practical challenges and optimizing the performance of PV modules in real-world conditions.

Conflicts of Interest

The authors declare no conflicts of interest regarding the publication of this paper.

References

[1] https://circuitglobe.com/photovoltaic-or-solar-cell.html

[2] https://www.cleanenergyreviews.info/blog/solar-panel-components-construction

[3] https://sinovoltaics.com/learning-center/materials/solar-glass-applications-and-co

mparison-to-light-trapping/

[4] https://www.abovesurveying.com/what-you-should-know-about-solar-pv-module-backsheet-failure/

[5] https://couleenergy.com/datasheet-values-rating-of-a-solar-panel/

[6] http://solarcellcentral.com/limits_page.html

[7] Faiman, D. (2008) Assessing the Outdoor Operating Temperature of Photovoltaic Modules. *Progress in Photovoltaics*: *Research and Applications*, **16**, 307-315. https://doi.org/10.1002/pip.813

[8] Skoplaki, E. and Palyvos, J.A. (2009) On the Temperature Dependence of Photovoltaic Module Electrical Performance: A Review of Efficiency/Power Correlations. *Solar Energy*, **83**, 614-624. https://doi.org/10.1016/j.solener.2008.10.008

[9] Mattei, M., Notton, G., Cristofari, C., Muselli, M. and Poggi, P. (2006) Calculation of the Polycrystalline PV Module Temperature Using a Simple Method of Energy Balance. *Renewable Energy*, **31**, 553-567. https://doi.org/10.1016/j.renene.2005.03.010

[10] Lee, Y. and Tay, A.A.O. (2012) Finite Element Thermal Analysis of a Solar Photovoltaic Module. *Energy Procedia*, **15**, 413-420. https://doi.org/10.1016/j.egypro.2012.02.050

[11] Usama Siddiqui, M., Arif, A.F.M., Kelley, L. and Dubowsky, S. (2012) Three-Dimensional Thermal Modeling of a Photovoltaic Module under Varying Conditions. *Solar Energy*, **86**, 2620-2631. https://doi.org/10.1016/j.solener.2012.05.034

[12] Zhou, J., Yi, Q., Wang, Y. and Ye, Z. (2015) Temperature Distribution of Photovoltaic Module Based on Finite Element Simulation. *Solar Energy*, **111**, 97-103. https://doi.org/10.1016/j.solener.2014.10.040

[13] Marwaha, S., Pratik, P. and Ghosh, K. (2018) Thermal Model of Silicon Photovoltaic Module with Incorporation of CFD Analysis. *Silicon*, **14**, 4493-4499. https://doi.org/10.1007/s12633-021-01184-3